JOURNAL OF MATERIALS SCIENCE **34** (1999) 1543–1552

Rheological properties of poly(acrylamide)-bentonite composite hydrogels

DEYU GAO
Institute of Technical Physics, Heilongjiang Academy of Sciences, Harbin, Heilongjiang, People's Republic of China

R. B. HEIMANN
Department of Mineralogy, Freiberg University of Mining and Technology, D 09596 Freiberg, Federal Republic of Germany, and Department of Chemical and Materials Engineering, University of Alberta, Edmonton, Alberta, T6G 2G6, Canada

M. C. WILLIAMS
Department of Chemical and Materials Engineering, University of Alberta, Edmonton, Alberta, T6G 2G6, Canada

L. T. WARDHAUGH
NOVA Chemicals Ltd., Calgary, Alberta, T2E 7K7, Canada

M. MUHAMMAD
D.B. Robinson Research Ltd., 9419-20 Ave. Edmonton, Alberta, T6N 1E5, Canada

Dynamic and transient rheological properties were measured for a series of hydrogel composites whose microstructure has been reported previously. These hydrogels, composed of radiation-crosslinked polyacrylamide and bentonite clay particles acting as polymer-absorbing mechanical crosslink sites, were prepared in the range 50–95% water. Dynamic storage and loss moduli (G', G'') were obtained at several strain amplitudes, over a range of frequency (ω) from 10^{-2} to 10^{2} rad/s. Step strains produced stress peaks and decays interpreted in terms of the stress relaxation modulus, carried to 10^{4} s. Rheological complications with possible slip, yielding, and nonlinearities were avoided but are discussed in detail. Rubberlike rheology was exhibited in general, and G' found to depend exponentially on solids content, with parameters only weakly dependent on ω. A practical measure of gel strength, defined in terms of the size of a water-containing cube that is mechanically stable, is used to demonstrate that these gels have considerable strength, with even a 1-m cube stable at 80% water.

1. Introduction

Hydrogels, known for their anomalous capacity to absorb water while retaining the physical properties of soft solids, have gained great attention in recent years. This is due to the wide range of applications to which they have been put, and their potential for novel uses in the future. Among these applications are diapers [1] biomedical devices such as surgical implants, skin grafts, and soft contact lenses [2]; buried communication cables [3], plugs for enhanced oil recovery operations, additives to concrete [4], and sensors known as "smart polymer gels" responding to environmental stimuli such as light [5], pH [6, 7], temperature [8], and electric fields [9].

Most commonly, hydrogels are composed of lightly crosslinked polyelectrolytes such as polyacrylamide or polyacrylic acid. The extent of crosslinking is usually the factor in determining both swelling capacity and mechanical strength. As with most rubbery crosslinked materials, an increased crosslink density increases all measures of hydrogel strength and stiffness, such as the static elastic shear modulus G, measured at constant shear strain γ [10], and the dynamic shear storage modulus G' [11], measured in sinusoidal oscillating strain $\gamma^{\circ} \sin \omega t$ (where ω is the frequency of oscillation, t is time and γ° the strain amplitude). This effect of crosslinking to achieve strength must necessarily limit the ability of the polymeric network to expand when imbibing water, so that one expects an inverse correlation between G or G' and swelling capacity. This was demonstrated for a series of polyacrylic acid-based superabsorbers [12]. While the crosslink density can be controlled during the production process, and the equilibrium extent of swelling can be related to crosslink density theoretically [10], the complexities of polyelectrolyte hydrogels require that experimental methods be invoked to determine both swelling and strength parameters for each case.

A complementary technique for influencing both swelling and strength of chemically crosslinked

hydrogels is to add clay particles to create hydrogel composites [13]. While this creates greater complexity in these systems, it also adds another degree of control over properties. In particular, greater strength can be achieved and product costs can be reduced, a feature especially important for large-scale engineering applications such as it enhanced oil recovery. Our laboratory (U of A) has recently investigated a set of materials of this hydrogel-composite class, composed of crosslinked polyacrylamide mixed with bentonite particles. The microstructural character of these composites was reported earlier [14]. Briefly, the polyacrylamide molecules were found to be intercalated into the lamina of clay in bimolecular layers. We therefore expect the clay particles to serve as both reinforcing fillers and additional (mechanical) crosslink sites in the polymer network. Several important properties were also reported earlier [14], such as a strong resonse to changes in pH and electric field strength. However, no attention was given there to the practical questions of mechanical strength and viscoelasticity.

Here, we deal with several measures of mechanical and viscoelastic strength for the bentonite/polyacrylamide composite hydrogels. Both G' and its companion G'' (loss modulus) are presented, as well as the transient stress modulus G^+ associated with a sudden strain imposed upon the material at rest, and carried out to long times as is typical in stress relaxation testing to determine relaxation modulus $G_r(t)$ [11]. All rheological properties are reported as functions of water content (i.e., a measure of swelling). The independent mechanical variables for G' and G'' are γ° and ω, while the transient step-strain modulus G^+ is tested for several γ and tracked for almost six decades of t, so $G^+ \to G_r(t)$.

2. Experimental

2.1. Materials

Monomers *N*,*N*-methylene bisacrylamide (MBAM) and acrylamide (AM) both identified as Electrophoresis Reagent, were obtained from Isolab Inc. These components, as well as sodium hydroxide (Mallinckrodt Canada Inc.) and sodium bentonite (Avonlea, Saskatchewan) were used as received, without further purification.

2.2. Sample preparation

Samples containing water contents of 95, 85, and 50% were all prepared by post-treatment of a base hydrogel containing approximately 70% water, whose manufacture and microstructure were described earlier [14]. Briefly, the latter hydrogel was created from a dense non-settling suspension of bentonite clay particles in distilled water (30% w/w clay) with pH adjusted to about 10.5 with NaOH. To this was added an equal amount of 30% w/w AM solution in water, (with stirring, to ensure homogeneity), the resulting suspension containing 30% solids and 70% water. After two hours of soaking, to permit the AM to intercalate with the clay particles, MBAM was added (2%) with further mixing, and the suspension then purged with N_2 gas to displace oxygen. Polymerization and crosslinking were induced by electron-beam irradiation of energy 9 Mev, at Whiteshell Research Centre, Atomic Enery of Canada. The subsequent gel composite had the consistency of a strong rubbery solid, with 68% water and 32% solids (clay plus the two acrylamide monomers), and served as the base hydrogel.

This mateial was converted into the test samples as follows. For the 85% and 95% water cases, the necessary additional water was placed in contact with the base hydrogel for ten days at room temperature, sufficient for the imbibition process to absorb the added water, distribute it uniformly, and achieve swelling equilibrium. For the 50% water case, the base hydrogel was dried in an oven to a weight corresponding to removal of the water necessary to achieve the targeted concentration.

For all the hydrogel composites, specimens for rheological testing were cut by hand with a razor blade, into a disk shape of approximate thickness 2 mm and diameter 50 mm, then transferred to airtight plastic bags to prevent loss of water by evaporation prior to rheological testing. Several samples were prepared for each water content, to enable replicate testing.

2.3. Apparatus

Rheological measurements were made with a Rheometrics Mechanical Spectrometer, Model 800 (RMS800) fitted with a 2–2000 g Force Rebalance Transducer (FRT) to sense the material torque responses under strain. Samples were contained between two horizontal parallel stainless steel platens of 50 mm diameter. In the RMS 800, the lower platen is driven to achieve the desired strain program $\gamma(t)$ in the sample. The upper platen in such testing remains stationary, transmitting torque from the sample to the FRT. Data are converted to the relevant material properties by computer software integral to the testing system. Material strain is reported as $\gamma = \theta R/h$, where $\theta(t)$ is the programmed angular displacement of the lower platen, R is platen radius, and h is the controlled separation of the platens (here, $h \cong 2$ mm). While the γ-measure is actually the strain at the outer rim (γ_R) and γ is not uniform in the sample (varying with radial position, from 0 at the center to the maximum γ_R), the measured torque is completely dominated by conditions at the greatest radial position so that $\gamma \cong \gamma_R$ is a good rheological parameter to associate with shear stress and resulting torque measurements, and generally is used when reporting results from such testing.

Because the hydrogel composites were wet to the touch, despite their solid-like behavior, it was determined to avoid or minimize the possibility of sample slippage on the steel platens. A layer of abrasive paper was therefore glued to both platens prior to loading each sample. The modified surfaces, with the waterproof "wet and dry" abrasive paper (United Abrasives Inc., Willimantic, CT, USA, grade 400A, particle size 21–24 μm) were found in preliminary tests to be superior to use of unaltered steel surfaces alone.

2.4. Procedures

Samples were removed gently from their airtight bags and laid onto the lower platen in a concentric position,

after which the upper platen was lowered until contact was made at approximately $h = 2$ mm. The uneven thickness of hand-cut samples led to uneven contact with platen surfaces, suggesting that more uniform surface contact might result by moving the upper platen further downward, exerting a small compression that would deform the uneven regions laterally. This was indeed possible for the samples of 95 and 85% water content, for which material was squeezed outward beyond the platens by 3–5 mm and then trimmed off. The samples with only 50% water were too stiff to be compressed enough to achieve this outflow, but were also trimmed to align with the platen rim.

In this sample configuration, the only mechanism for moisture loss during testing is evaporation from the sample/air surface at the platen rim. Such moistrue loss would cause increasing local solids concentration, and because of its location at $r = R$, a disproportionately high reading of torque. This potential problem was overcome by two precautions: (a) coating the free surface with a thin layer of silicone oil (moisture barrier) of viscosity sufficiently low to have no effect on torque measurements, and (b) closing an oven attachment around the platens and placing water-soaked tissues within it, thus saturating the atmosphere around the samples and eliminating humidity gradients that might drive the evaporation.

Linear viscoelastic properties are defined to characterize material sensitivity to time and rate variables i.e., $G'(\omega)$ and $G^+(t)$ and thus must be independent of nonlinearities in the form of residual dependency on testing parameters such as γ and γ°. It was therefore necessary to detemine what range of γ° or γ would be sufficiently small so that nonlinearities would not appear, while using strain amplitudes as large as possible so that stress responses of the samples would also be large and could be measured easily and accurately. These compromises are often found in the strain range of 1–10%, but must be found empirically for each material. In the present testing, G' was first measured at fixed ω (0.1 rad/s) for a wide range of γ° (to be shown below), from which it was found that G' was γ°-independent for samples with 95% water if $\gamma^\circ \leq 10\%$, and for samples with 85% water if $\gamma^\circ \leq 5\%$. For samples with 50% water, it was difficult to find a γ° sufficiently small to give a truly linear response (as will be demonstrated below), so that $\gamma^\circ = 0.1\%$ and 0.2% were chosen arbitrarily for further ω-testing; use of smaller γ° did not produce material stresses large enough to measure. A similar investigation for $G^+(t)$ found most results to be independent of γ after the initial rapid stress build-up, so that in the stress relaxation regime ($t \geq 0.03$ sec) $G_r(t)$ showed little γ-dependency: this is also displayed below.

3. Results

3.1. Strain sweeps

Measurements of G' at $\omega = 0.1$ rad/s for a range of γ° covering almost four orders of magnitude are shown in Fig. 1 for all three materials. The feasible γ°-ranges cited above were inferred from these data. The curve for 50% water appears superficially to achieve a linear limit (absolute flatness at low γ°), but such is not the case, as is discussed below. Although G'' are not displayed here, it is relevant to comment that $G'' \ll G'$. Since these properties are defined in the context of complex numbers, in terms of the complex modulus [11] $G^* \equiv G' + iG''$, it is clear that the absolute value of G^* (determined by stress amplitude) is dominated by the storage modulus, $|G^*| \cong G'$. This is one indicator of the solidlike nature of the hydrogel composites, since a more fluid-like material would be characterized by viscous behavior (energy loss by viscous dissipation) so G'' would be larger and contribute more substantially to $|G^*| = [(G')^2 + (G'')^2]^{1/2}$.

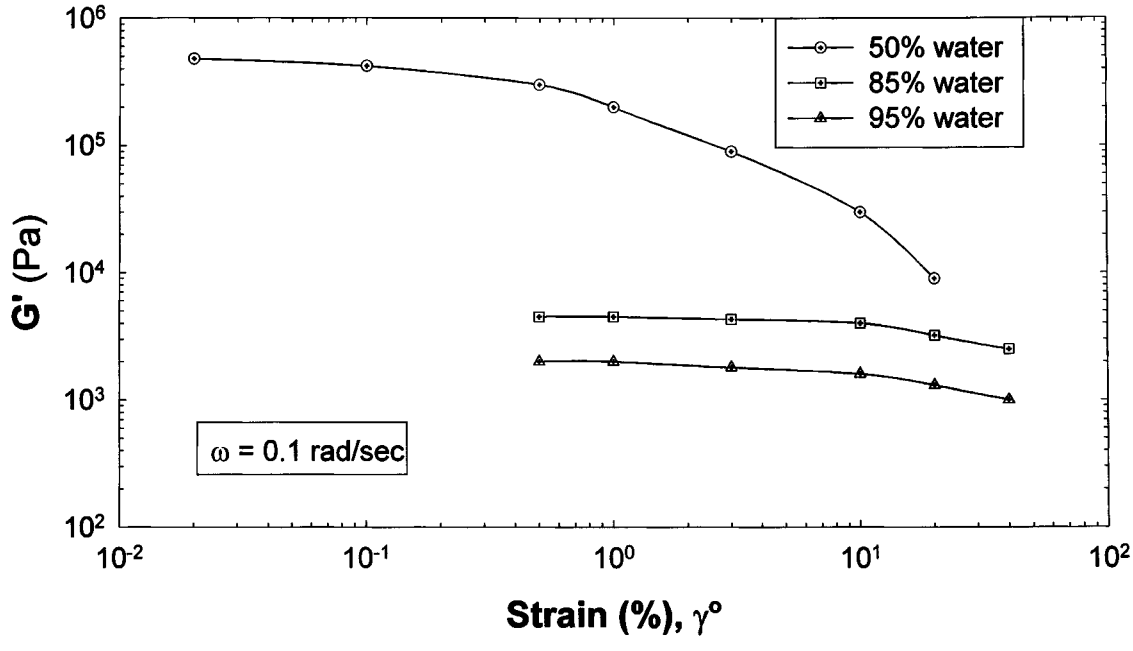

Figure 1 Strain sweeps to determine onset of nonlinearities in dynamic testing, where strain is controlled as $\gamma = \gamma^\circ \sin \omega t$. Frequency was $\omega = 0.1$ rad/s for all materials, while strain oscillation amplitude γ° varied. Both platens of the parallel-plate shearing assembly were modified by a coating of "wet-and-dry" abrasive paper.

An alternative interpretation [11], of stress data in dynamic testing is in terms of a pair of viscosity parameters, $\eta'(\omega)$ and $\eta''(\omega)$, with the dynamic viscosity η' and η'' being related to a complex viscosity η^* by $\eta^* = \eta' - i\eta''$. Basic definitions require that $\eta' = G''/\omega$, and $\eta'' = G'/\omega$, so that only one set of properties (say, G' and G'') needs to be reported for complete characterization of the linear viscoelastic behavior of a given material. These definitions also require that $|\eta^*| = |G^*|/\omega$. Given the dominance of G' over G'' for these materials, it is useful to note that $|\eta^*| \cong G'/\omega$ so that Fig. 1 ($\omega = 0.1$ rad/s) results for G' can be used to give approximately $|\eta^*| \cong G'/\omega = 10G'$ and is rigorously converted to $\eta'' = 10G'$.

3.2. Frequency sweeps

The plots of $G'(\omega)$ and $G''(\omega)$ are given for polyacrylamide/bentonite hydrogels in Fig. 2, with Figs 2a, b, and c representing samples with water contents of 95,

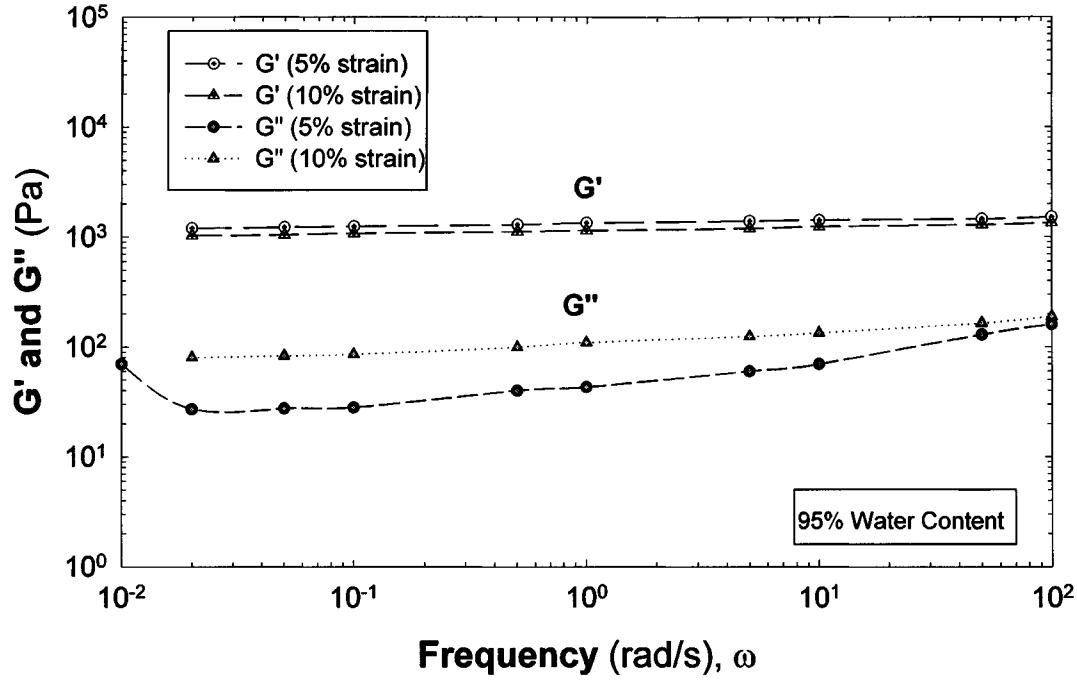

(a)

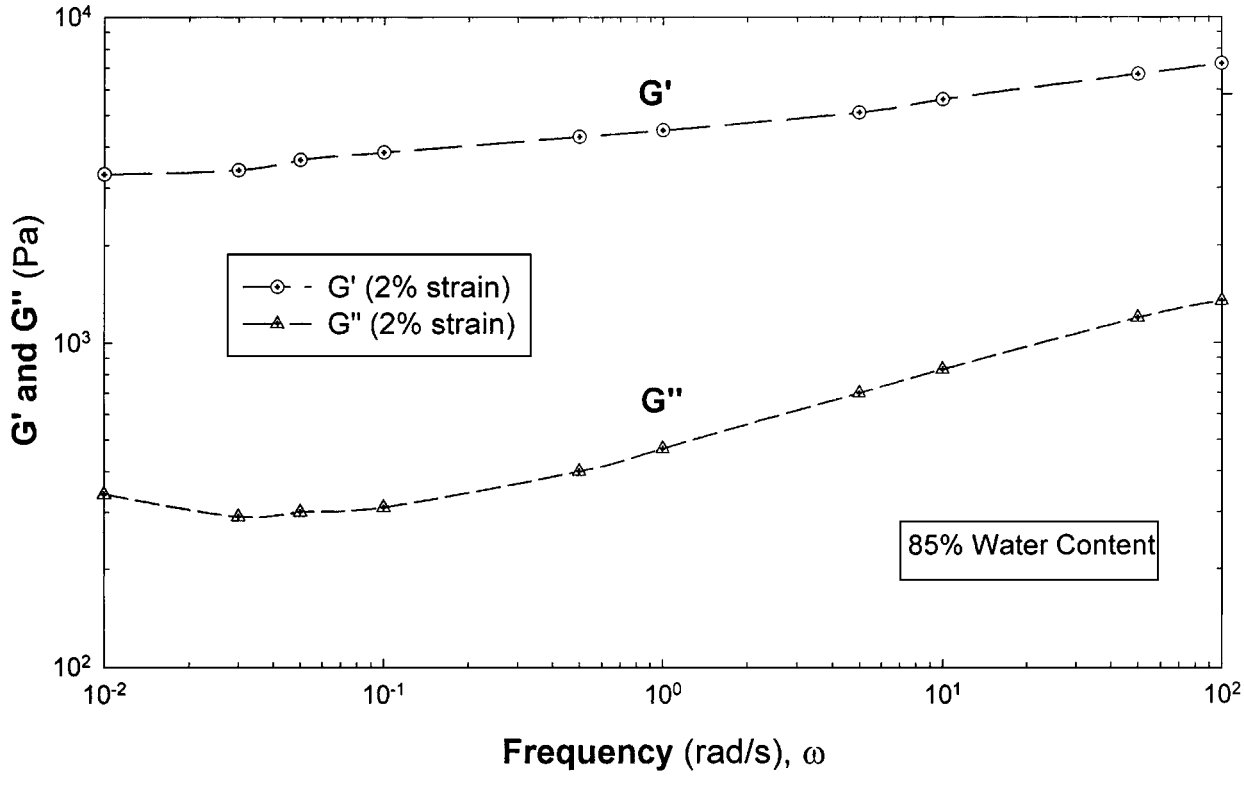

(b)

Figure 2 Frequency sweeps, ω-dependence of G' and G'' for all materials. Several strain amplitudes γ° were used to assess the possible influence of nonlinear effects, as shown on each figure. (a) 95% water. (b) 85% water and (c) 50% water. (*Continued*).

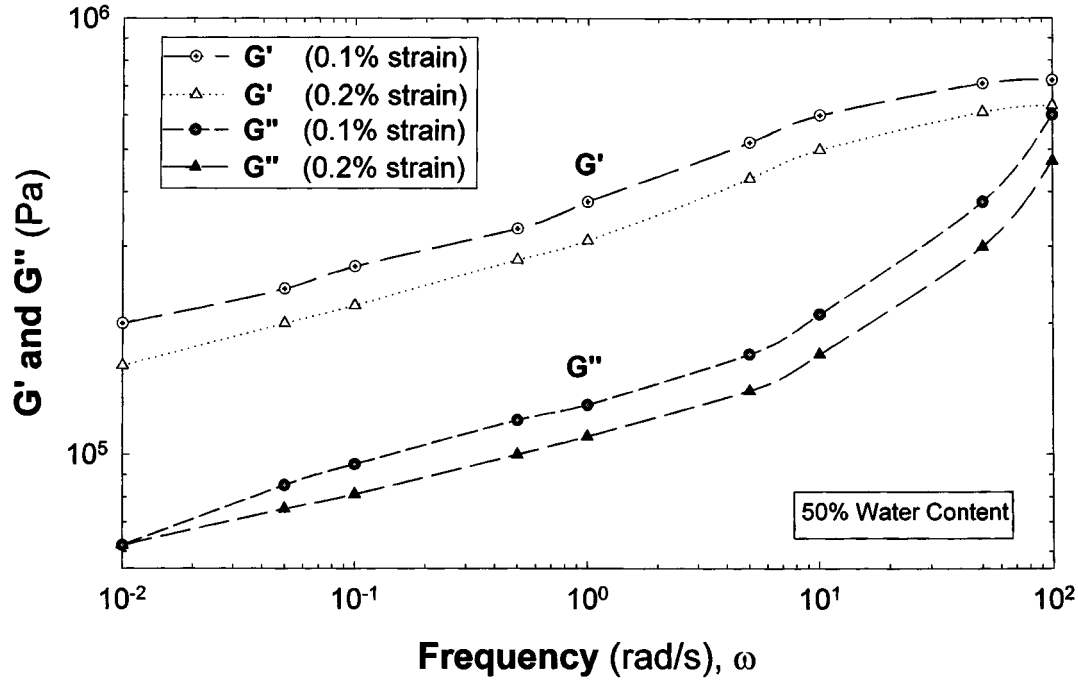

(c)

Figure 2 (*Continued*).

85, and 50%, respectively. For 95% water, results are displayed for two strain amplitudes, $\gamma^\circ = 5$ and 10%. These plots confirm that $G' \gg G''$, as stated above, but show a slight difference between the two γ°. This demonstrates that the case $\gamma^\circ = 10\%$ was just barely into the nonlinar testing regime (see Fig. 1), and that the $\gamma^\circ = 5\%$ data in Fig. 2a are more reliable for representing linear viscoelasticity. All testing for 85% water samples was done at $\gamma^\circ = 2\%$, so the possible influence of nonlinearities cannot be assessed, but from the results of Figs 1 and 2a might be assumed to be small. However, for 50% water content (Fig. 2c), the use of $\gamma^\circ = 0.1$ and 0.2% do not lead to exact superposition of results, which shows some nonlinearities still to be present, so that the $\gamma^\circ = 0.1\%$ data should be regarded as more representative of linear behavior. Fig. 1 agrees, for the 50% water samples, that $\gamma^\circ = 0.1\%$ is almost down into the fully linear regime, but that $\gamma^\circ = 0.2\%$ is not.

The impressive strength (or "stiffness") of these materials is indicated by the magnitudes of $G'(\omega)$ in Fig. 2, inasmuch as the value of G' for the majority component (water) is $G' = 0$. The fact that $G' \gg 0$ reflects a substantial presence of true solids (clay and rubber), and also the existence of a network structure, composed of the crosslinked polymer and the clay linkage sites [14]. The flatness of the three $G'(\omega)$ curves indicates that these network structures are very stable when exposed to a wide range of perturbation frequencies, even though the effective rate of shear ($\dot{\gamma}^\circ = \omega\gamma^\circ$) also covers seveal orders of magnitude. Clearly, the materials do not disassemble at any frequency (as long as the applied stress magnitude is low). Regardless of the high water content, the gels do not flow like fluids until a true rheological yielding occurs, when the network is torn apart by higher applied stresses that exceed the yield stress. Such yielding was not examined explicitly in this study, but is discussed in later passages below.

Inspection of Figs 2a, b, and c collectively reveals unexpected behavior in the ratio $G''/G' = \tan\delta$, where δ is the phase difference between the oscillating $\gamma(t)$ imposed and the responding material stress $\tau(t)$. For 95 and 85% water cases, $\tan\delta \cong 0.1$, which could be interpreted as a surprisingly high degree of "relative fluidity" in view of the fact that these materials were phenomenologically solid-like bodies. Dropping the water content to 50% led to an abrupt jump of $\tan\delta$ to the range 0.4–0.5. This jump is better understood in terms of the solids concentrations (c) passing from the semidilute regime ($c = 5\%$ and 15%) to the concentrated solids regime ($c = 50\%$); under these circumstances $\tan\delta = 0.4$–0.5 could still be considered surprisingly high "fluidity."

The ω-dependence of $G''(\omega)$ in Fig. 2 is not close to flat, but it is not expected to be. If we regard the hydrogel volumes as composed primarily of water (50–95%, here), energy dissipation (i.e., energy loss) effects might be thought to be controlled by the viscosity of water ($\eta_w = 10^{-3}$ Pa·s). Since $G'' = \eta'\omega$, the approximation $G'' \cong \eta'_w\omega$ (perhaps useful at extremely low solids content) shows that some ω-dependence in G'' is required. The enhancement of G'' above the extremely low approximation for water ($G''_w = 10^{-3}\omega$ Pa) implies that a major contribution is being made by the viscous component of the network (clay particle linkages, plus crosslinked polycacrylamide) at the prevailing solids concentration, $G'' \equiv \eta'(c)\omega$. The expected behavior of $\eta'(\omega, c)$ is to have a steep drop-off ("ω-thinning") as ω increases beyond negligible values. This behavior results in the appearance of the minimum in $G''(\omega) = \eta'(\omega) \times \omega$ observed in Figs 2a and b.

Although Fig. 2c exhibits no minimum, the $G''(\omega)$ curve displays a concave-up shape arising from the same superposition of dual contributions to G'': [decreasing $\eta'(\omega)$] $\times$ [linearly increasing ω].

The fact that $G''(\omega)$ generally shows an increase (and not a ω-thinning) with ω increases over four orders of magnitude demonstrates that the hydrogels retain excellent mechanical energy-damping ability over a wide frequency range. Moreover, that ability is enhanced over that of the water component abone by several orders of magnitude, despite the anticipated "ω-thinning" of the solids component over the same frequency range.

3.3. Stress start-up/relaxation transients

The shear stress transient $\tau^+(t, \gamma)$ is used to define the transient modulus (relaxation modulus G_r) $G_r = G^+(t) = \tau^+/\gamma$, so presentation of $G^+ = (t)$ also suffices to convey τ^+ when γ is given. These moduli are displayed in Fig. 3, for all three water-content cases. For 95% water content, the use of two strains ($\gamma = 5\%$, 10%) produced identical results for $t > 0.03$ s, with only a minor difference in the short-term oscillation in the first 0.02 s. There is somewhat greater nonlinearity displayed for samples with 85% water, as becomes apparent at long times, where the data for $\gamma = 5\%$ and 10% diverge slightly for $t > 20$ s. However, even at $t = 2000$ s the difference is only about 3% in $G^+ = G_r(t)$. Based on these results for water contents of 95 and 85%, the case for 50% water was tested only at $\gamma = 5\%$; no short-term oscillation at short times could be detected. For all three materials, the $\tau^+(t)$ transients peaked at about $t = 0.02$ s, for all γ.

4. Discussion

4.1. Ranges of kinematic variables

The linear viscoelastic properties have been measured over a wide range of time and rate variables, with t in $G^+(t)$ tests covering t from 10^{-2} to 2000 s (over 5 orders of magnitude) and ω in $G'(\omega)$ tests ranging from 10^{-2} to 10^2 (4 orders of magnitude) The onset of nonlinearities was found at lower γ for the firmer materials (e.g., $\gamma^\circ = 0.2\%$ for G' in samples with 50% water, but $\gamma^\circ = 10\%$ for samples with 95% water, with similar results for γ in G^+ tests). These strain values are within normal ranges, but the reasons for the onset of those nonlinearities is not clear. At sufficiently large γ all materials must exhibit rheological nonlinearities, and with polymeric systems this can arise when the polymer coils are substantially distorted from their rest state of spherical symmetry, isotropy, and Gaussian mass distribution,

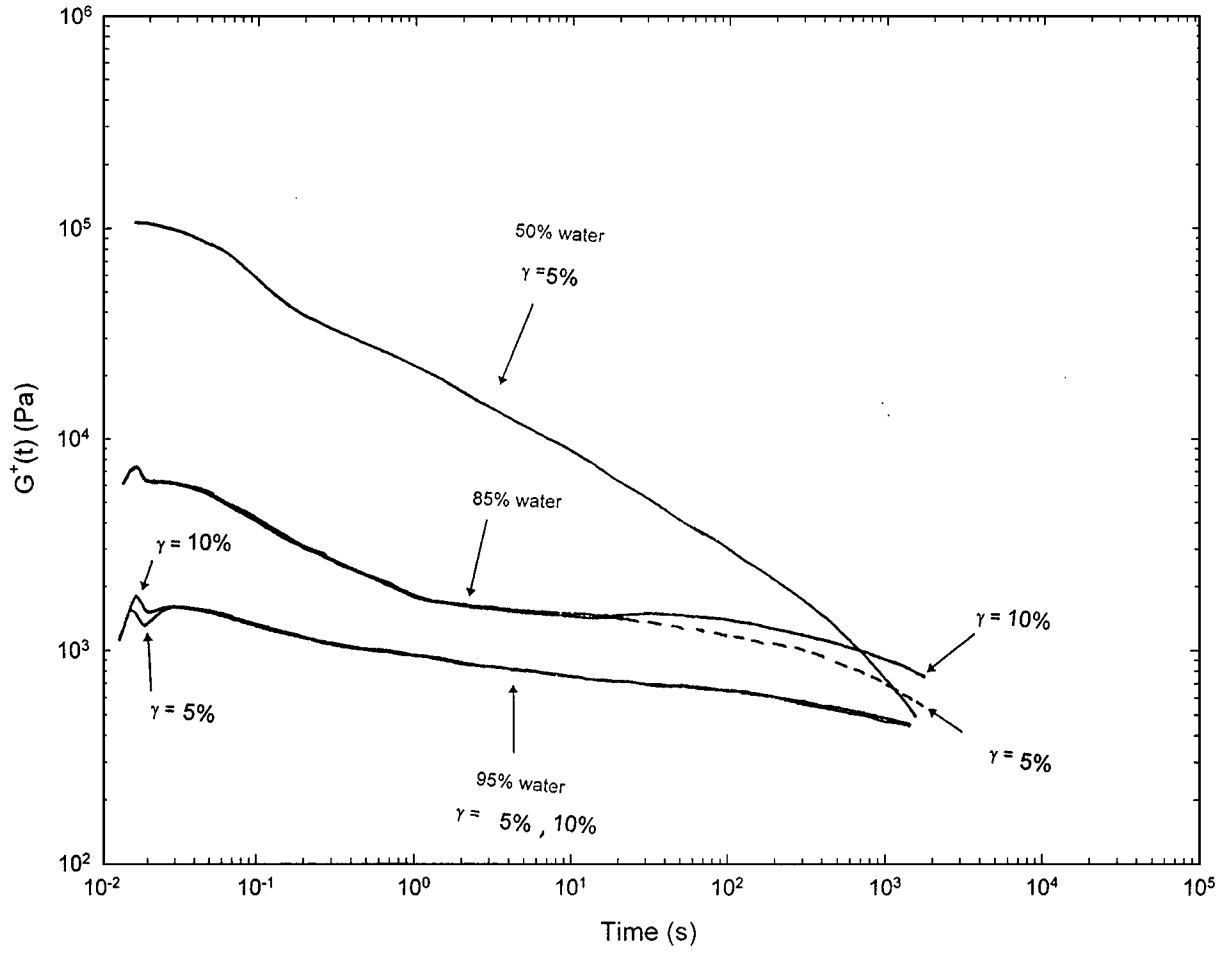

Figure 3 Transient shear modulus $G^+ \equiv \tau^+/\gamma$ for the start-up shear stress τ^+ response of materials upon imposition of a shear strain γ abruptly upon a state of rest. When values peak and begin to decline, $G^+(t)$ becomes equivalent to the stress relaxation modulus, $G_r(t)$. Several strain amplitudes were used to assess the possible presence of nonlinearities. The three materials and the γ employed are identified on the figure.

to assume ellipsoidal symmetries and orientation. Additional factors arise in "structured" systems, when microscopic deformations can break down or otherwise alter the microstructure even when molecular-level nonlinearities are negligible. This is most likely the case for the hydrogel/clay composites, but further investigation remains to verify this.

4.2. Concentration dependence

A major objective of this study was to determine how the water content affected the various viscoelastic strength parameters. It is sometimes helpful to represent this dependence in terms of the materials solids content (c) which includes both clay and polyacrylamide in equal amounts. This is demonstrated by comparing the set of three curves for $G'(\gamma^\circ; c)$ in Fig. 1 and for $G^+(t; c)$ in Fig. 3. The anticipated increase of modulus with c is clearly shown there, over the whole range of γ and t. The same result emerges for $G'(\omega; c)$ over the whole range of ω as observed by inspection of Figs 2a, b, and c collectively. This c-dependence is made more explicit in Fig. 4, where $G'(c)$ is displayed for both the low-ω regime ($10^{-2}\,s^{-1}$) and the high-ω regime ($10^{2}\,s^{-1}$). In both regimes, the data plotted on semilog coordinates are essentially linear, signifying exponential dependence on c:

$$G'(\omega; c) = G'_0(\omega)e^{Ac} \tag{1}$$

where $A(\omega)$ determines the slopes in Fig. 4 and G'_0 is the intercept at $c = 0$. Because the $c = 0$ limit corresponds mathematically to both no clay and no polymer, the interpretation of G'_0 must be made carefully. The zero-polymer limit would normally give $G' = 0$ (no elasticity), but in fact we find that $G'_0 > 0$. We suspect this result is a consequence of sample preparation procedure, wherein acrylamide polymerization and crosslinking are completed before the post-treatment steps of adding water or removing water were performed. Thus, the extrapolated $c = 0$ limit (or, 100% water) does not have its usual significance, and the material performs viscoelastically in this limit. This also explain why G'_0 is weakly ω-dependent as well; the two lines in Fig. 4 give $G'_0 = 8.5 \times 10^2$ and 7.5×10^2 Pa at $\omega = 10^2\,s^{-1}$ and $10^{-2}\,s^{-1}$, respectively. The closeness of these two values is consistent with the matrix behaving as a crosslinked rubbery network, which should exhibit a broad $G'(\omega)$ plateau in a certain middle range of ω so that only a minor sensitivity to ω should be expected to appear (increasing weakly with ω, as found here). The exponential c-dependence of $G'(\omega; c)$ in Fig. 4, and likewise the corresponding viscosity parameter $\eta''(\omega; c) = G'/\omega$, is probably a manifestation of the clay component of the solids. Equation 1 resembles strongly the functional form for enhancement of concentrated suspension viscosity by rigid particulates of irregular shape [15]. To make the resemblance more complete, Equation 1 would have to be re-cast in terms of clay volume fraction (ϕ) and the maximum packing fraction (ϕ_{max}). This would make Equation 1 capable of extrapolation more reliably to the high-ϕ limit ($\phi \to \phi_{max}$), whereas its current form does not increase with c fast enough to represent the enormous G' values expected at higher c as $c \to c_{max}$.

4.3. Critical solids content

Even though the samples tested here were clearly solid-like and did not flow spontaneously as fluids, this class of hydrogel composites could have an unacceptably low

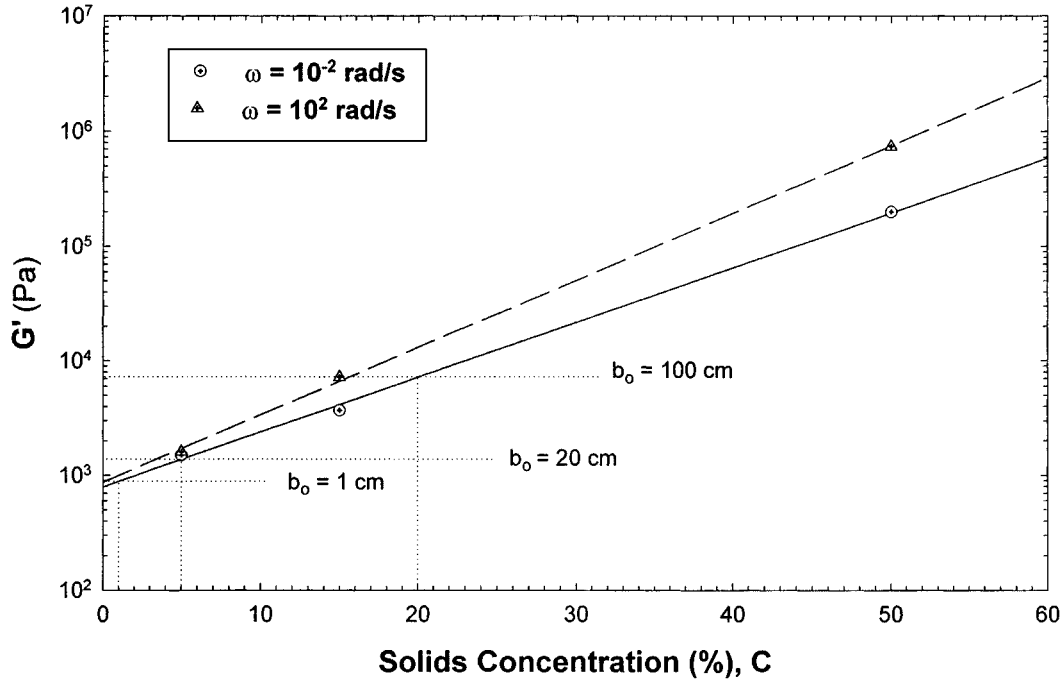

Figure 4 Dependence of G' on solids concentration, c. The ω-sensitivity of this relationship is demonstrated by showing $G'(c)$ for the lowest $\omega(10^{-2}$ rad/s) and highest ω (10^2 rad/s) employed in this study; for all other ω, results are intermediate. Values of b_0 correspond to the largest size of a material cube of a given solids concentration that is stable (see text).

strength for various technical applications. In the absence of yield stress measurements, the data on $G'(c)$ could be used to evaluate the adequacy of the strength of a given material or to estimate the solids concentration needed to fabricate a composite for a given service requirement.

It is first necessary to define the critical amount of deformation or strain that can be tolerated in service (say γ_{crit}) and then determine whether the stress (τ) encountered in service can cause $\gamma > \gamma_{crit}$. Expressed in terms of a static modulus, this leads to the concept of the critical modulus that permits the critical strain $G_{crit} = \tau/\gamma_{crit}$. By identifying the low-ω storage modulus in Fig. 4 and Equation 1 with G, we thus can obtain G'_{crit} and the corresponding required solids contents c_{crit}.

This general technique will now be used to demonstrate in practical terms the "solidity" of these hydrogels. We consider a cube of dimension b_0 and accept its strength to be barely adequate if the force of gravity causes it to collapse only to a height b_1, the resulting body having unchanged volume $V = b_0^3$ and expanded lateral dimensions. The critical strain in compression is thus $\gamma_{crit} = \Delta b/b_0 = (b_0 - b_1)/b_0$. We define this condition as a collapse to half the original height, $b_1 = b_0/2$ so $\gamma_{crit} = 1/2$. Gravitational force on the original cube is $F = mg = \rho b_0^3 g$ (ρ = sample density), causing an initial compressive stress $\tau_0 = F/A_0 = F/b_0^2 = \rho b_0 g$ so that the critical compression modulus is $E_{crit} = \tau_0/\gamma_{crit} = 2\rho g b_0$. For incompressible materials, the unidirectional modulus (E) in compression or tension is related to the shear modulus (G) by $E = 3G$. We also identify the static shear elastic modulus G with the dynamic elastic storage shear modulus $G'(\omega)$ at low ω, from which we obtain $G_{crit} = G'_{crit} = 2\rho b_0 g/3$. Next, the $G'(c)$ relationship must be inserted. From Fig. 4 and Equation 1, $G'_{crit} = G'_0(\omega)\exp(Ac_{crit}) = 2\rho b_0 g/3$, from which $c_{crit} = (2.303/A)\log(2\rho b_0 g/3G_0)$.

This result, using the density of water, is superimposed on Fig. 4. For a 1-cm cube, unacceptable solidity ($\gamma_{crit} = 1/2$) corresponds to solids content below $c \cong 1\%$. Our highest-water-content sample ($c = 5\%$) was sufficiently "solid" to conform to this criterion, as no slumping was observed with either the test specimens ($b_0 = h = 0.2$ cm) or the larger bulk materials ($b_0 > 5$ cm). At $c = 5\%$, G' is found to be about 1300 Pa (see Fig. 4) and this equals G_{crit} when $b_0 = 3G'/2\rho g = 20$ cm. Considering a much larger object, using the same γ_{crit} criterion, we select $b_0 = 1$ m and find that such a cube would be stable ($\gamma < 1/2$) for $c \geq 20\%$, predicting that a hydrogel composite of this composition could securely retain an enormous volume of water. Our general observations of the $c = 15\%$ samples tested here (which should be slightly weaker than the $c = 20\%$ examples cited above) certainly confirm the "solidity" of that material when handled as specimen disks of diameter 5 cm and thickness 0.2 cm, with the additional impression that a body of dimension 1 m made of the same material would not have been stable (in agreement with these calculations). Similarly, handling the $c = 50\%$ material impressed us that it would easily have been stable if 1 m in size.

4.4. Time and rate effects in viscoelasticity

Linear viscoelastic properties are expected to depend on t and $1/\omega$ in equivalent ways—i.e., $G'(\omega)$ should have the same value as $G_r(t)$ when $t = 1/\omega$. This principle can be tested by using Figs 2 and 3 together. We select arbitrarily $t = 10^2$ s in Fig. 3, corresponding to $\omega = 10^{-2}$ rad/s in Fig. 2.

The comparison of $G'(10^{-2})$ with $G_r(10)^2$ shows good agreement for 95% water samples ($G' = G_r = 1200$ Pa) and for 85% water samples ($G' = G_r = 3700$ Pa) but not for 50% water samples. For the latter, $G'(\omega = 10^{-2}\text{s}^{-1}) = 2 \times 10^5$ Pa, while $G_r(t = 10^2\text{s}) = 4500$ Pa. This discrepancy is discussed below.

4.5. Experimental complications

4.5.1. Loading trauma

The practice of squeezing the hand-cut disk between the platens, to the point where radial flow occurred, succeeded in distributing the material to all radial positions and filling the gap completely; thus, defects in specimen smoothness and nonuniformities in cut dimensions did not lead to certain artifacts for the squeezed samples (95 and 85% water). However, the flow process itself signifies that the solid-like material structure was altered by this technique, which implies that subsequently measured properties were not precisely those of the originally prepared samples. To evaluate the importance of this factor, we note that the 50% water specimens could not be compressed in this way, so their strucuture remained unchanged. While defects due to non-flatness of 50% water specimens could have caused other problems, the data of Fig. 4 indicate that the same $G'(c)$ correlation fits yielded and non-yielded specimens alike. This would be highly unlikely if either the loading trauma of one or the non-flat character of the other were severe enough to produce major artifacts in $G'(\omega)$. Moreover, $G^+(t)$ evidence shows that the samples that flowed the most during loading (95 and 85% water) exhibited the greatest long-term retention of strength in stress relaxation. Fig. 3 shows that a long-time near-horizontal plateau expected for strongly structured network systems is displayed by the 95 and 85% water samples but not the 50% water samples, even though the latter suffered no loading trauma. Thus, again, the case of 50% water seems anomalous, though unquestionably having far greater strength than the others. We will subsequently ascribe both apparent anomalies to the $G^+(t)$ behavior in the transient/relaxation tests of 50% water samples.

4.5.2. Slip

The surface wetness of hydrogel samples always makes rheological measurements complex, sometimes aggravated by such practices as the present compression-loading of samples with 95 and 85% water. One consequence of a water layer between the sample and the platens is a $G'(\gamma^\circ)$ anomaly in strain sweeps. In such cases, the water acts as a lubricant and prevents the platens from actually deforming the sample to a true strain equal to that commanded by the RMS 800

software i.e., equal that expected from the true platen motion. Consequently, the computed $G'(\gamma^\circ)$ curve will exhibit a drop-off at prematurely small γ° and descend very rapidly. Such behavior was seen here in preliminary tests (mentioned above) with 95% water samples. Several trial modifications were made to the smooth platen surfaces, but only the wet-and-dry abrasive paper was successful in eliminating this anomaly in $G'(\omega;\ \gamma^\circ)$ testing. The curves for different platen surfaces were displaced vertically from each other, another indicator of slip because sample deformation should be independent of surface variations if all adhered well to the samples. Another feature of that study was an apparent h-dependence in computed values of $G'(\gamma^\circ)$ when the whole set of data for different surfaces (with minor variations in h) were examined. This is also believed to be a manifestation of slip and presumably removed from all later G' data by use of the abrasive paper. Indirect evidence for that removal is, again, the success of the $G'(c)$ correlation in Fig. 4, which would not have emerged if measurements were reflecting only the resistance of water films for all samples (nor would the magnitude of G' have been so large).

Only in the case of long-time sustained strain and stress do we believe some slip might have influenced the data presented here—i.e., in the G_r results. The short-time G^+ data contain oscillations which suggest elastic effects, not the purely viscous effects expected from a water film, so $G^+(t)$ for $t < 0.05$ s are presumed essentially free of slip effects. At long times, to $t > 2000$ s, the high-water samples retain high G_r values as is characteristic of normal relaxation phenomena for crosslinked systems, so slip is believed to be absent there too. However, for 50%-water samples (Fig. 3) no plateau is seen, and a near-steady drift downward persists to $= 10^4$ s. It seems likely that this reflects the slow recoil of the sample over a film of water, after an initial large deformation caused by the high stresses transmitted through the same film by rapid platen displacement at $t = 0$.

Therefore, the two anomalies cited above in connection with the 50%-water sample are believed to reflect a long-term slip on a film of water in the $G_r(t)$ tests. However, slippage on a water film would be difficult to distinguish from slip over a low-viscosity layer of the test material itself, which had yielded (become fluid) next to the platen as a consequence of exposure to high initial stresses, exceeding its intrisic yield stress, τ_y. See below.

4.5.3. Yield stresses

Although high-water samples experienced a yielding in compression when being loaded, this information is not easily transformed into data on possible yield stresses in shear deformation. Moreover, if yielding was induced during G' and G^+ tests, the interpretation of those latter results could be influenced by the consequent flow processes, so we conclude with a few remarks about τ_y in shear. The $\tau^+(t)$ data that can be reconstructed from Fig. 3 show peak values τ_{max} that depend on γ, since $\tau = G^+\gamma$. If these exceeded τ_y for any material, then some portion of that "yielded" material, probably near the surface of the driving platen, woud thereafter behave as a low-viscosity fluid until such time as it could repair itself by Brownian or other thermodynamic processes. We believe that these self-repairing processes occurred very swiftly following the compressive loading and squeezing-flow phenomena imposed on the high-water-content samples, which is why they subsequently responded as normal intact viscoelastic materials, in dynamic and relaxation testing. Some information about τ_y can be inferred from the $\tau^+(t)$ tests. For 95%-water content samples, Fig. 3 shows good superposition of the curves for $\gamma = 5$ and 10%, indicating that either both cases yielded or neither did. Retention of high-G_r plateaus for both suggests that neither did, meaning that τ_{max} for $\gamma = 10\%$ (130 Pa) is less than τ_y. This, in turn, can be used to assess whether the dynamic testing with oscillating stress amplitude $\tau^\circ \cong |G^*|\gamma^\circ$ had τ° small enough so that τ_y was not exceeded during stress oscillation. From Fig. 2a, for $\gamma^\circ = 5\%$ we get $\tau^\circ \cong (1500\ \text{Pa})\,(0.05) = 75$ Pa, which is clearly well under the bound $\tau_y > 130$ Pa. Also from Fig. 2a, for $\gamma^\circ = 10\%$, $\tau^\circ \cong (1200\ \text{Pa})\,(0.1) = 120$ Pa, which is also low enough to avoid yielding during oscillation. These two conclusions are consistent with the superposition of the $G'(\omega)$ data for $\gamma^\circ = 5$ and 10% in Fig. 2a. A similar argument for the 85% water samples, if one regards Fig. 3 as evidence of good superposition of the $\gamma = 5$ and 10% curves, is $\tau_y > 580$ Pa. The $G'(\omega)$ data in Fig. 2b were taken at $\gamma^\circ = 2\%$ and had a maximum value at $\omega = 10^{-2}$ s^{-1}, $\tau^\circ = (7200\ \text{Pa})\,(0.02) = 144$ Pa, well below the 580 Pa bound for τ_y. However, the relaxation behavior in Fig. 3 could be interpreted as showing that some yielding had occurred, as the curves for $\gamma = 10$ and 5% diverged at long times. The peak stresses for those cases were 580 and 300 Pa, respectivley, leading to the inference that $300 < \tau_y < 580$ Pa. The previous conclusion about the $G'(\omega)$ results being free of yielding remains valid under these circumstances.

For the 50%-water data, the $G^+(t)$ tests were made only at $\gamma = 5\%$, and the possible yielding is ambiguous because of possible slip on a water film. With only one γ employed in measuring G_r, we have no guidance from relaxation data about whether τ_{max} (3600 Pa) exceeded or fell short of τ_y. Instead, we seek guidance from $G'(\omega)$ data in Fig. 2c, where the abrasive paper secured a non-slip condition. Those data do not show superposition for the two τ° employed. While it is not possible to discern whether that lack of superposition is due to $\tau^\circ > \tau_y$ or merely ordinary large-strain rheological nonlinearity, we will dismiss the latter possibility on the grounds that the strains are quite small (0.1 and 0.2%) and do not normally cause nonlinearities in other crosslinked rubbery materials. Since the non-superposition in Fig. 2c is apparent even at the lowest $G' \approx G^*$ values (i.e., at $\omega = 10^{-2}$ rad/s), we will postulate that yielding has occurred there for one or both of the two γ°-cases. For $\gamma^\circ = 0.1\%$ we have $G' \cong 2.3 \times 10^5$ Pa, and for $\gamma^\circ = 0.2\%$ $G' = 2.0 \times 10^5$ Pa. Thus, $\tau^\circ = 2.3 \times 10^4$ Pa and 4.0×10^4 Pa, respectively. If values this large are needed to cause yielding in oscillatory shear, it is highly doubtful that values only about 10% of that (i.e., $\tau_{max} = 3600$ Pa) in the $G^+(t)$ tests could cause yielding there. The conclusion is that the downward drift of

$G_r(t)$, with no rubbery plateau, is not a consequence of yielding behavior but rather the deformation of the sample (less than the command γ) by means of stresses imposed through a film of water and subsequent recoil and loss of deformation along the same film at long times. If correct, this assessment means that numerical values presented for $G^+(t)$ in Fig. 3 and cited here for τ_{max} represent the true rheology of the 50%-water hydrogel only approximately. An earlier indication of the importance of the water film in permitting slip was the discovery that G^+ at $t = 100$ s (4500 Pa) was far lower than G' at $\omega = 1/t = 10^{-2}$ rad/s (about 2 to 4×10^4 Pa), which we now find was not caused by a yielding and flow of the 50%-water hydrogel.

4.5.4. Reproducibility of results

An enormous range of factors can be considered here, beginning with sample and specimen preparations, specimen loading practices, and RMS tests on those specimens. In the latter case, such data as G' measured in γ°-sweeps and ω-sweeps can be repeated on the same loaded specimen with reproducibility of 2–5%. These two types of sweeps, to give $G'(\gamma^\circ; \omega)$ and $G''(\gamma^\circ, \omega)$ as well as the transient modulus data $G^+(\gamma, t)$, were always made on the same specimen, without re-loading. When a fresh specimen is involved, the task is more difficult and can be addressed by examining the linear-property values η'_0 as the low-γ° limit of $\eta'(\gamma^\circ)$, identical to the low-ω limit of the $\eta'(\omega)$ curve at constant γ°. Only one such duplicate trial was made, using the 95%-water sample. In that case, with the abrasive paper in place on the platens to prevent slip, the two specimens that were used were not cut identically and were not perfectly flat or smooth; both required some vertical pressure and outflow to secure good surface contact and complete gap filling, and thus suffered loading trauma to differing degrees. The final gap spacings were 2.621 mm and 2.263 mm. The corresponding values of η_0 were 13400 Pa · s and 13000 Pa · s, respectively. This difference is only 3%, within the range of RMS accuracy itself.

For a given loaded sample, the data of Figs 2b and c could be reproduced within the RMS capabilities, 2–5% or better.

There were no replicate trials with sample preparation in this study. One question which arises concerns the internal consistency of adjusting the water content in two different ways .. i.e., by hydration vs. dehydration of the stock 70% hydrogel. While we have no proof that the two processes gave equivalent results (and there are reasons why they might not), we can point to Fig. 4 as evidence for consistency. If these two preparative processes led to significantly different microstructures and properties, it seems unlikely that data for all three concentrations would have produced such well-behaved colinear points (Fig. 4) and the simple exponential c-dependence of Equation 1. Again, we believe the two fabrication methods are equivalent within 5% here.

Overall, we believe these data and these methods are reproducible within 5% with the composite hydrogels studied here.

5. Conclusions

1. The clay/polyacrylamide composites have the capacity to absorb large amounts of water while retaining good mechanical strength and high damping characteristics, and therefore represent a new and promising class of hydrogel materials.

2. The strengthening effect of the clay concentration was found to be exponential, $G' = G'_0 \exp(Ac)$, over a wide range of frequencies of sinusoidal dynamic testing, with a weak ω-dependence appearing as $G'_0(\omega)$ and $A(\omega)$. Further work is needed to explore the factors determining A.

3. Measurements of viscoelastic properties faced certain obstacles (slip and yielding during tests, loading trauma, etc.) that were recognized and overcome in ways that should prove useful to others working with hydrogel rheology in shearing deformation.

4. Internal consistency checks of data on $G^+(t)$ and $G'(\omega)$ at various strain levels were shown to be capable of establishing approximate values of τ_y or bounds on τ_y.

Acknowledgements

Financial support for this work was provided by a contract between The Institute of Technical Physics, Harbin, P.R.C. and The Alberta Research Council, Edmonton (for D.G. and R.B.H.) and by an operating grant from the Natural Sciences and Engineering Research Council of Canada (for L.T.W, M. M, and M.C.W.). We are indebted to Drs. John W. Barnard and Ajit Singh of Whiteshell Laboratories, AECL Research, Pinawa, Manitoba for granting access to their electron-beam irradiation facility.

References

1. F. L. BUCHHOLZ, *Trends Polym. Sci.* **2** (8) (1994) 277.
2. L. L. HENCH and E. C. ETHRIDGE, "Biomaterials. An Interfacial Approach," (Academic Press, New York, 1982) pp. 47–49.
3. H. POLLE, European Patent Application EP 375 685 (1990).
4. D. GAO, R. B. HEIMANN and S. D. B. ALEXANDER, *Adv. Cement Res.* **9** (1997) 93–97.
5. A. SUZUKI and T. TANAKA, *Nature* **346** (1990) 345.
6. R. A. SIEGEL and B. A. FIRESTONE, *Macromolecules* **21** (1988) 3254.
7. L. B. PEPPAS and N. A. PEPPAS, *Chem. Eng. Sci.* **46** (1991) 715.
8. T. G. PARK and A. S. HOFFMAN, *J. Appl. Polym. Sci.* **46** (1992) 659.
9. T. TANAKA *et al. Science* **218** (1982) 467.
10. P. J. FLORY "Principles of Polymer Chemistry" (Cornell University Press, Ithaca, New York, 1953).
11. J. D. FERRY, "Viscoelastic Properties of Polymers," 2nd ed. (John Wiley and Sons, Toronto, 1970).
12. K. A. BRANDT, S. A. GOLDMAN and T. A. INGLIN, US Patent 4 654 039 (1987).
13. B. K. G. THENG, "Formation and Properties of Clay-Polymer Complexes," (Elsevier, Amsterdam, 1974).
14. D. GAO and R. B. HEIMANN, *Polymer Gels and Networks* **1** (1993) 225.
15. C. R. WILDEMUTH and M. C. WILLIAMS, *Rheologica Acta* **24** (1985) 75.

Received 17 October 1997
and accepted 26 October 1998